

# Analysis of SAXS data from ionomer systems

D. J. Yarusso\* and S. L. Cooper

Department of Chemical Engineering, University of Wisconsin, Madison, WI 53706, USA

(Received 6 February 1984)

A model was proposed earlier for the microstructure of ionomers which attributes the small-angle X-ray scattering (SAXS) peak observed in these materials to interparticle interference between small ionic domains arranged in the hydrocarbon matrix with a liquid-like degree of order. In this work, that model is used to interpret SAXS results obtained for a number of different ionomer systems. In addition, the effect of swelling of sulphonated polystyrene ionomers with water is investigated using this approach. Finally, the effect of temperature on the scattering was studied. The results reveal some interesting differences in domain size between different ionomer systems. The ethylene/methacrylic acid ionomers contain very small domains consistent with the concept of a multiplet, while the sulphonated EPDM rubbers have rather large domains. The results of the water absorption studies were inconsistent with the assumption that there is no change in the number of ionic domains upon swelling but if that assumption is not made, the data can be rationalized with the model. The elevated temperature measurements demonstrated the stability of the ionic domains even at temperatures well above those where the materials can be processed, leading to speculation regarding the mechanism of melt flow in ionomers.

(Keywords: ionomers; small-angle X-ray scattering; microstructure; domains; multiplet; swelling)

## INTRODUCTION

In a previous publication<sup>1</sup>, a model for the scattering of X-rays by ionomers was proposed. The model attributes the characteristic ionomer SAXS peak to interparticle interference between spherical ionic aggregates which are distributed in the matrix with a liquid-like degree of order. The correlation in their positions arises because there is a closest approach distance between any two particles. That distance depends on the diameter of the particles and the thickness of the layer of bound hydrocarbon material on the surface of the aggregate.

It has been argued that interparticle scattering models such as the one proposed by the authors are inconsistent with the observed dependence of the SAXS data on the degree of swelling of the ionic domains with water. As other authors have pointed out, if one assumes that there is no change in the number of aggregates upon swelling, then the observed Bragg spacing should change in the same proportions as the macroscopic linear dimension change upon swelling<sup>2,3</sup>. The available data indicate that the Bragg spacing changes much more than the macroscopic dimensions<sup>4,5</sup>.

The authors previously pointed out that there is no compelling reason to assume that the number of aggregates is constant upon swelling and suggested that the proposed interparticle scattering model could be consistent with the swelling data if this variation were allowed<sup>1</sup>. In this work, the model was applied to SAXS data obtained on water swollen sulphonated polystyrene ionomer samples to test this hypothesis.

In addition, SAXS data were obtained for a number of other ionomer systems and analysed by applying the proposed model. This was done to determine the general

applicability of the model and to examine differences in aggregate structure as a function of the chemical structure of the ionomer.

Finally, X-ray data taken at elevated temperatures on several ionomers was also studied using this approach. It was hoped that the critical temperature for ionic aggregate dissociation predicted by Eisenberg<sup>6</sup> might be observed.

## EXPERIMENTAL

### Zinc sulphonated polystyrenes

The same sulphonated polystyrene starting materials described in the previous paper were studied here. The sample designations and compositions are summarized in Table 1. In the present work only highly neutralized salts were prepared. The samples were neutralized with zinc acetate by the same procedure as before with the exception that the powders were dried more vigorously prior to moulding. The neutralized powders were dried *in vacuo* for 24 h at 110°C rather than at 65°C. Samples were compression moulded as before at 200°C and then dried again *in vacuo* at 120°C for 24 h. The discs were cooled *in vacuo* to 25°C over a period of ~4 h and stored in a desiccator. Atomic analysis indicated that a neutralization level of 82% ± 4% was achieved.

To accomplish the swelling, the samples were exposed to 5, 10 or 15 psi steam in a pressure cooker and the amount of absorbed water determined by measurement of the weight gain. Typical exposure times were about 0.5 h.

### Rubidium, strontium and nickel sulphonated polystyrenes

Because of difficulty encountered with the previous method in recovering the polymer from solution, these salts were prepared by a different procedure. The acid

\* The 3M Company, St. Paul, MN, USA

form of the sulphonated polystyrene was dissolved in tetrahydrofuran at a concentration of  $100 \text{ g l}^{-1}$  and the solution was filtered as before. A stoichiometric amount of the neutralizing salt was dissolved in a small amount of water and added to the polymer solution. In this case the following salts were used for neutralization: rubidium acetate, nickel acetate tetrahydrate and strontium hydroxide octahydrate. Again, single phase neutralization was achieved. At this point the polymer solutions were poured into glass Petri dishes lined with aluminium foil and the solvent was evaporated, first in a fume hood at room temperature for about 48 h and then *in vacuo* at  $120^\circ\text{C}$  for 24 h. The polymer was ground into a powder using a mechanical mill and then moulded and annealed by the same procedure as described previously.

#### Zinc carboxylated polystyrenes

Four samples of carboxylated polystyrenes were obtained from Dr Adi Eisenberg at McGill University. The synthesis of these materials has been described by Lundberg and Makowski<sup>7</sup>. The samples were neutralized with zinc acetate dihydrate by the same procedure used for the rubidium, strontium and nickel salts of sulphonated polystyrene. The carboxylate contents for these samples are summarized in Table 2.

#### Ethylene/methacrylic acid ionomers

Three samples of ethylene/methacrylic acid copolymers (trade name Surlin<sup>R</sup>) neutralized with zinc were obtained from E. I. DuPont de Nemours and Company. The methacrylic acid content and degree of neutralization of these samples are listed in Table 3. These samples were compression moulded at  $180^\circ\text{C}$  and 55 MPa for 10 min and quenched to room temperature in  $\sim 60$  s.

#### Sulphonated EPDM rubber ionomers

Several samples of sulphonate ionomers prepared from a terpolymer of ethylene, propylene and a diene monomer (EPDM) were obtained from Dr Ilan Duvdevani of the Exxon Research and Engineering Company. The diene monomer used in these samples was ethylidene norbornane. A post polymerization sulphonation reaction was used to attach a sulphonic acid group to the diene monomer unit in the chain. The synthetic procedures are described by Makowski *et al.*<sup>7</sup>. The sulphonate content and cation content of these samples are listed in Table 4. Since the exact composition of the polymer backbone is unknown, these levels cannot be presented in the same

Table 1 Sulphonated polystyrenes

| Sample | Mole fraction sulphonated |
|--------|---------------------------|
| A      | 0.0168                    |
| B      | 0.0337                    |
| C      | 0.0555                    |
| D      | 0.0691                    |

Table 2 Carboxylated polystyrene compositions

| Sample | Mole fraction carboxylated repeat units |
|--------|---|
| A      | 0.0310                                  |
| B      | 0.0396                                  |
| C      | 0.0584                                  |
| D      | 0.0782                                  |

Table 3 Zinc ethylene/methacrylic acid sample characterization

| Sample  | Mole fraction methacrylic acid | Fraction of acid groups neutralized |
|---------|--------------------------------|-------------------------------------|
| B-10864 | 0.043                          | 0.21                                |
| B-10865 | 0.043                          | 0.57                                |
| 4489-1  | 0.055                          | 0.59                                |

Table 4 Sulphonated EPDM sample characterization

| Sample  | Sulphonate level (meq./100 g) | Counterion                             | Counterion content (meq./100 g) |
|---------|-------------------------------|--|---------------------------------|
| GL-44-B | 30                            | $\text{FeOH}^{2+}$ and $\text{NH}_4^+$ | 20                              |
| GL-46-A | 30                            | $\text{Fe}^{2+}$                       | 20                              |
| GL-47-C | 30                            | $\text{Eu}^{3+}$                       | 37                              |
| TP-303  | 30                            | $\text{Zn}^{2+}$                       | 60                              |

way as for the other ionomers studied. The polymers were received as films approximately 2 mm thick and were used without modification.

#### SAXS measurements and data analysis

All of the SAXS curves were obtained with a compact Kratky scattering camera and a position sensitive detector at the University of Wisconsin. An Elliot GX-21 generator was the source of  $\text{CuK}\alpha$  incident radiation. Monochromatization was accomplished using a nickel filter and pulse height discrimination. The scattering camera has a sample to detector distance of 60 cm and an effective detector length of 8 cm for a  $q$  range of  $6.0 \text{ nm}^{-1}$  to  $0.2 \text{ nm}^{-1}$  ( $q$  is the magnitude of the scattering wavevector defined as  $4\pi/\lambda \sin \theta$  where  $2\theta$  is the angle between the incident and the transmitted radiation). The detector length was divided into 128 effective channels for a resolution of about  $0.05 \text{ nm}^{-1}$ .

The data were corrected for detector sensitivity variations, parasitic scattering by the camera and sample cell, and absorption of the beam by the sample. The beam profile along the slit length was measured and the data were desmeared using the iterative method of Lake<sup>8</sup> and the measured slit length weighting function. The absolute scattering power in terms of  $I/I_0V$  was obtained by comparison of the intensity to that of a calibrated Lupolen<sup>R</sup> polyethylene sample corrected and desmeared by the same procedure.

The background scattering was determined by fitting the exponential relation of Rathje and Ruland<sup>9</sup> to the high  $q$  region of the data where the contribution from the multiphase structure has become negligible. That function was then subtracted from the data. The high temperature data were obtained by enclosing the sample in a temperature controlled cell with Mylar<sup>R</sup> windows. The measurements of the swollen samples were made in a sealed cell also with Mylar<sup>R</sup> windows to prevent loss of the water since the normal sample cell is exposed to rough vacuum. The effect of scattering by the sample cell was accounted for by subtracting the scattering of the cell from the sample scattering after correction for the beam attenuation by the sample.

A sample from the previous study was analysed to check the reproducibility of data between the Oak Ridge facility and the facility at the University of Wisconsin used here. The reproducibility in curve shape is excellent but the absolute amplitudes differ by about 20% with the UW

data giving the higher value. This difference is somewhat larger than the normal limits of such measurements<sup>10</sup>.

## RESULTS AND DISCUSSION

### Review of scattering model for ionomers

The model proposed in a previous paper by the authors consists of identical spherical ionic aggregates dispersed in the hydrocarbon matrix which may contain some ionic species<sup>1</sup>. The correlation in the relative positions of the different aggregate particles is determined by a hard sphere type of interparticle potential. However, the hard sphere interaction radius is larger than the radius of the scattering particle. The physical interpretation which was suggested is that the hydrocarbon chains which are necessarily bound to the ionic aggregates would provide a steric barrier to the closest approach of two aggregates but would not provide any scattering contrast. The equation for the scattering from such a system is a variation on the simple hard sphere model. We have chosen to use the equation derived by Fournet<sup>11-13</sup> based on the thermodynamic theory of Born and Green<sup>14</sup>. If the closest approach distance between two aggregates is  $2R_{CA}$  and the scattering particle radius is  $R_1$ , the scattered intensity is given by:

$$I(q) = I_e(q) V \frac{1}{v_p} v_1^2 \rho_1^2 \Phi^2(qR_1) \frac{1}{1 + \frac{8v_{CA}}{v_p} \epsilon \Phi(2qR_{CA})}$$

where

$$v_{CA} = \frac{4}{3} \pi R_{CA}^3$$

and

$$v_1 = \frac{4}{3} \pi R_1^3$$

$I$  is the intensity of scattered radiation,  $I_e$  is the intensity scattered by a single electron under the experimental conditions.  $V$  is the volume of sample illuminated by the incident beam. The electron density difference between the particles and the matrix is  $\rho_1$  and the average sample volume per particle is  $v_p$ .  $\epsilon$  is a constant very close to one and the function  $\Phi$  is defined by:

$$\Phi(x) = 3 \frac{\sin x - x \cos x}{x^3}$$

This model is shown schematically in Figure 1.

### Water absorption studies

As was mentioned in the Introduction, the behaviour of the SAXS patterns of ionomers upon swelling of the ionic domains with water has been used as evidence against morphological models which attribute the characteristic SAXS peak to interparticle interference. This argument is based on the assumption that there is no change in the number of ionic aggregates upon swelling. It is true that the intraparticle scattering models such as the depleted zone core-shell model which were reviewed previously<sup>1</sup> can explain the variation in the SAXS pattern with water swelling with this assumption. This was shown by Fujimura *et al.*<sup>5</sup> and by our own attempts to fit the data on the swollen sulphonated polystyrene samples with such a model. However, our earlier work found other problems

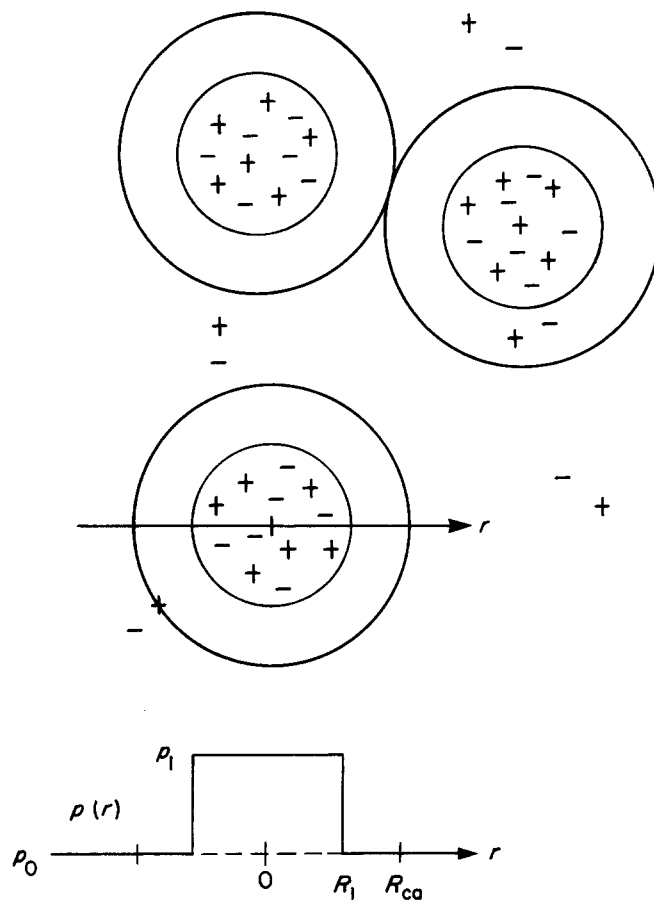


Figure 1 Schematic of modified hard sphere model and corresponding electron density profile for one of the particles

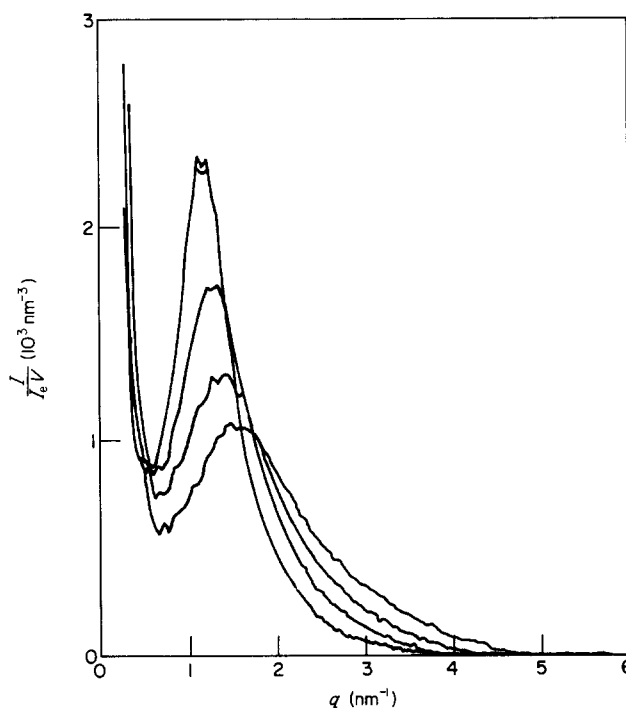
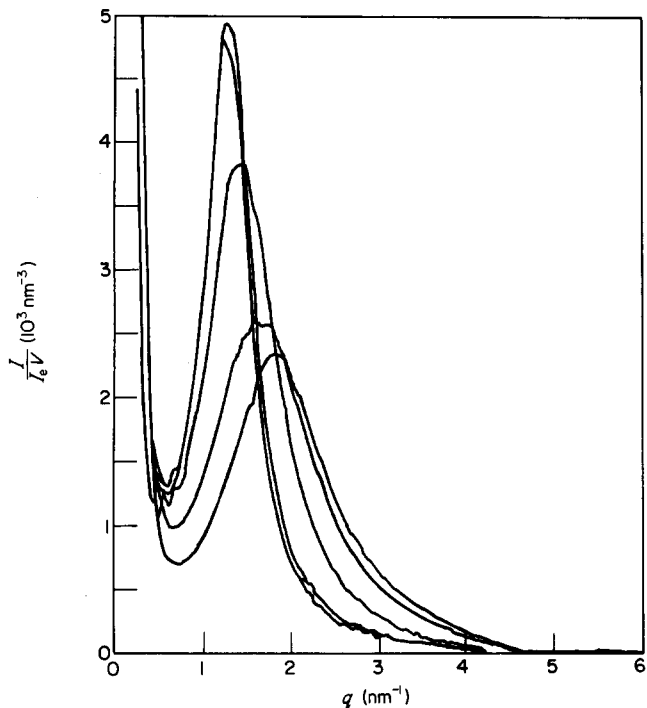
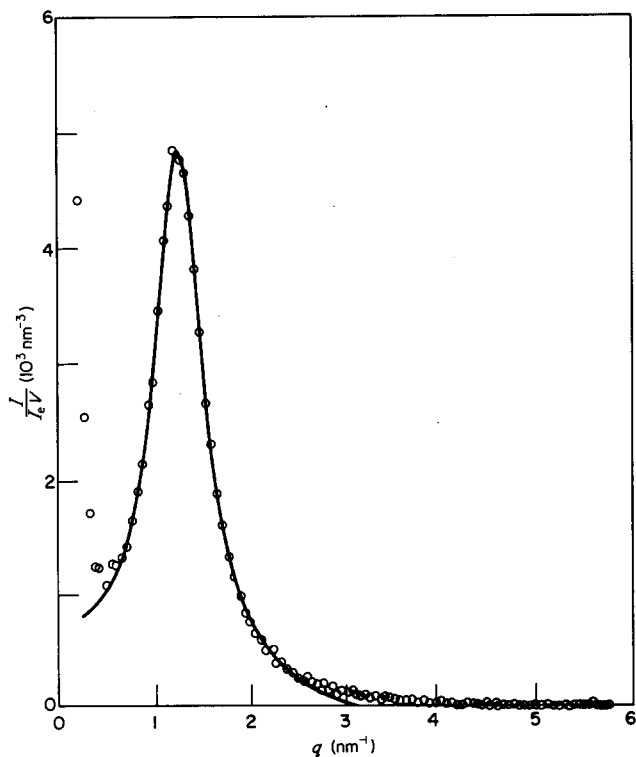


Figure 2 SAXS curves for Zn SPS B as a function of water content. The peak moves toward smaller  $q$  and sharpens as the water content increases

with such a model, namely that the variation in the aggregate volume and the depleted zone volume did not match the expected material balance as the overall ion content of the ionomer was changed.



**Figure 3** SAXS curves for Zn SPS D as a function of water content. The peak moves toward smaller  $q$  and sharpens as the water content increases



**Figure 4** Examples of fit of the modified hard sphere model to the data (circles) of water swollen Zn SPS sample D (7.6 wt%  $H_2O$ ). Model parameters are listed in Table 5

Therefore, the present study was undertaken to address the question of whether or not the proposed model could be consistent with the swelling data if one allowed for the possibility of a rearrangement of the ionic species and a change in the number of ionic domains. Rather than assuming that the number of domains would remain constant during swelling and looking only at the apparent Bragg distance, it was decided to use the information from

the model fitting regarding the aggregate volume and the concentration of aggregates to see if it was consistent with the amount of water added.

The SAXS curves of the sulphonated polystyrene samples as a function of water absorption level are shown in Figures 2 and 3. An example of one of the model fits is shown in Figure 4. The best fit parameters are listed in Table 5. Next a comparison is made between the microscopic changes in volume fraction of aggregates and that expected based on the amount of water added. Figures 5 and 6 show the microscopic degree of swelling as indicated by the change in the volume fraction of aggregates from the control sample plotted against the change expected based on the amount of water added. The latter

**Table 5** Model fit parameters for water swelling

| Water content<br>(% of original mass)                   | $\rho_1$ ( $nm^{-3}$ ) | $R_1$ (nm) | $R_{CA}$ (nm) | $v_p$ ( $nm^3$ ) |
|---|------------------------|------------|---------------|------------------|
| <i>Zinc sulphonated polystyrene, 3.37% sulphonated:</i> |                        |            |               |                  |
| 0   | 133                    | 0.82       | 1.62          | 71               |
| 1.2   | 105                    | 0.97       | 1.81          | 97               |
| 2.0   | 76                     | 1.13       | 2.05          | 100              |
| 3.1   | 55                     | 1.31       | 2.28          | 102              |
| 3.7   | 54                     | 1.32       | 2.30          | 103              |
| <i>Zinc sulphonated polystyrene, 6.91% sulphonated:</i> |                        |            |               |                  |
| 0   | 116                    | 0.82       | 1.47          | 28               |
| 2.0   | 118                    | 0.91       | 1.59          | 43               |
| 3.5   | 87                     | 1.10       | 1.89          | 55               |
| 5.7   | 56                     | 1.32       | 2.14          | 59               |
| 7.6   | 51                     | 1.36       | 2.16          | 60               |

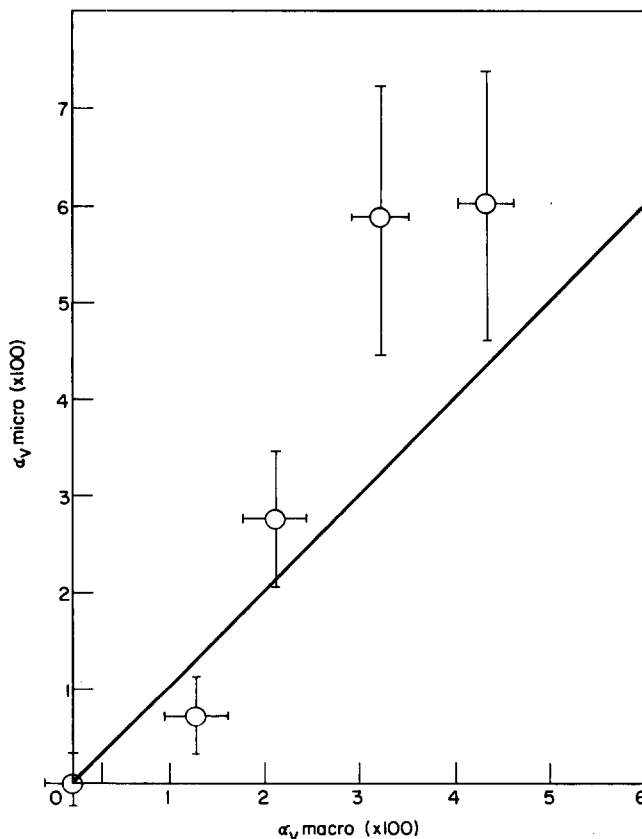


**Figure 5** Microscopic change in aggregate volume fraction vs. change expected based on macroscopic volume of water added.  $\alpha_v(\text{micro})$  is the volume fraction of aggregates as indicated by the SAXS data ( $v_1/v_p$ ) minus the value for the control sample.  $\alpha_v(\text{macro})$  is the volume fraction of added water. Data for sample B

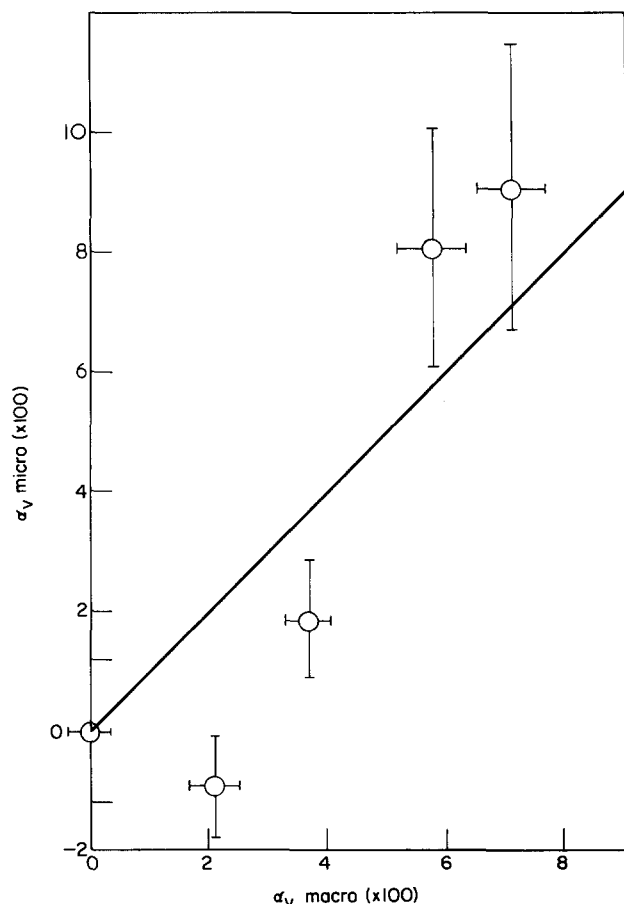


**Figure 6** Microscopic change in aggregate volume fraction vs. change expected based on macroscopic volume of water added. Data for sample D

is calculated assuming that the number of ions in aggregates is constant and that all the water added goes into the domains and takes up the same volume as the pure water. Using this approach, one finds that the discrepancy between the microscopic and macroscopic degrees of swelling, although present, is not nearly as great as when one assumes that there is no change in the number of aggregates as has been done in previous analyses. In fact one can see that the microscopic degree of swelling is not always larger than the macroscopic prediction as was found in the work of Fujimura *et al.*<sup>2</sup>. At low levels of swelling it is smaller.

The disagreement which exists could be the result of some of the assumptions mentioned above being invalid. In particular, the fraction of ions which are aggregated could change as well as the number of aggregates. Since it was calculated that initially only about half of the ionic groups are aggregated, the excess aggregate volume observed at high water contents could be due to aggregation of additional sulphonate groups. The lower values for the aggregate volume at low water contents may imply that in the early stages of absorption, the water is absorbed by the ionic groups which are in the matrix. Then at higher levels, those hydrated species tend to aggregate. Thus, the effect of water absorption on the scattering behaviour cannot be used to rule out interparticle scattering models if one accepts the possibility that the morphology may rearrange upon swelling resulting in a change in the number of aggregates and the number of ionic groups in each aggregate. The fact that the intraparticle scattering models can fit the data without

making these assumptions is not proof of the validity of those models but primarily a reflection of the fact that the aggregate concentration cannot be determined from the data for such a model and thus one can postulate a concentration which will make the results consistent with the model.

In comparing the results for the dry samples to those obtained on the corresponding samples in the previous study<sup>1</sup>, it can be seen that the ionic domains are smaller and the electron densities larger in this work. We expect that this is due to the more severe drying conditions employed here.

#### Other ionomer systems

In order to relate the results of the detailed work on the sulphonated polystyrene system to the existing ionomer literature, the SAXS curves of several other ionomers were measured and the proposed model was used to evaluate the ionic aggregate morphology in those materials.

The data along with the fits to the proposed liquid-like model are shown for some of these materials in Figures 7–11 and the resulting model parameters are listed in Table 6. (Note that the peak resulting from the polyethylene crystallinity is observable in the data for the ethylene/methacrylic acid ionomer at a  $q$  value of  $\sim 0.8 \text{ nm}^{-1}$ .) Even though the peak position and shape vary quite a bit for the different systems, the model is able to provide a good fit for all of them. Some interesting points emerge in these data. Firstly, the aggregate size is much smaller in the ethylene/methacrylic acid ionomers than in the sulphonated polystyrenes. The effective thickness of the layer of bound chains is lower for these materials also. This might be expected because of the greater flexibility of the polyethylene chains. The ionic domains and the bound layer thickness are both larger for the EPDM system. As expected, the concentration of particles is much lower for the EPDM based ionomers because the ion content is much lower.

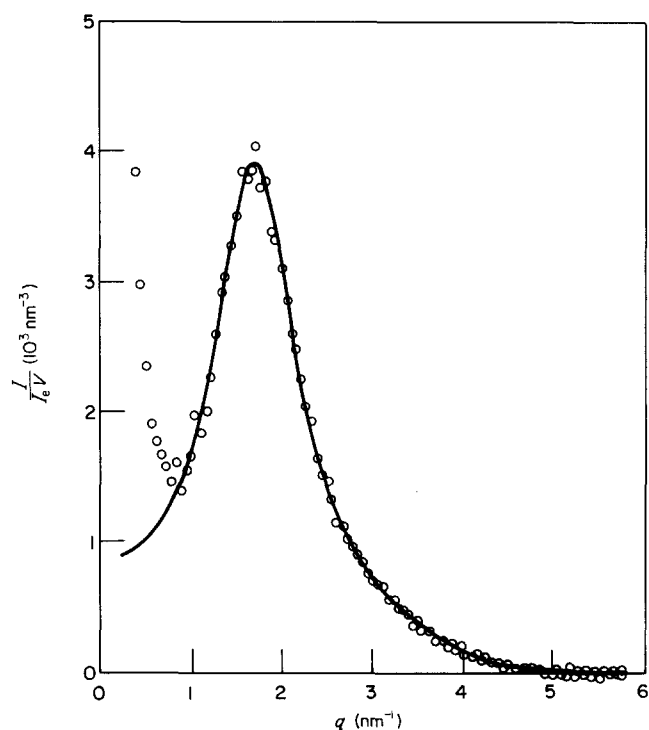


**Figure 7** SAXS curve and model fit for Rb SPS D

**Table 6** Model fit parameters for other ionomers

| Sample                     | $\rho_1$ (nm <sup>-3</sup> )           | $R_1$ (nm) | $R_{CA}$ (nm) | $v_p$ (nm <sup>3</sup> ) |
|----------------------------|--|------------|---------------|--------------------------|
| <b>SPS:</b>                |  |            |               |                          |
| Rb SPS A                   | 126*                                   | 0.98       | 1.67*         | 187                      |
| Rb SPS C                   | 126*                                   | 0.92       | 1.67          | 40                       |
| Rb SPS D                   | 126*                                   | 0.90       | 1.59          | 34                       |
| Sr SPS A                   | impossible to distinguish ionomer peak |            |               |                          |
| Sr SPS B                   | 131*                                   | 0.92       | 1.66          | 95                       |
| Sr SPS C                   | 132                                    | 0.89       | 1.60          | 48                       |
| Sr SPS D                   | 130                                    | 0.89       | 1.57          | 39                       |
| <b>CPS:</b>                |  |            |               |                          |
| Zn CPS A                   | 92*                                    | 0.82       | 1.40          | 145                      |
| Zn CPS B                   | 92*                                    | 0.78       | 1.41          | 87                       |
| Zn CPS C                   | 92*                                    | 0.78       | 1.36          | 50                       |
| Zn CPS D                   | 92*                                    | 0.77       | 1.30          | 44                       |
| <b>Surlyn<sup>R</sup>:</b> |  |            |               |                          |
| B-10864                    | 225*                                   | 0.44       | 0.63          | 26                       |
| B-10865                    | 225*                                   | 0.43       | 0.76          | 10                       |
| 4489-1                     | 225*                                   | 0.45       | 0.76          | 11                       |
| 4489-1-7                   | 225*                                   | 0.45       | 0.74          | 11                       |
| 4489-1-9                   | 225*                                   | 0.47       | 0.73          | 14                       |
| <b>EPDM:</b>               |  |            |               |                          |
| GL-44-B                    | 229                                    | 1.26       | 2.53          | 680                      |
| GL-46-A                    | 217                                    | 1.28       | 2.60          | 640                      |
| GL-47-C                    | 256                                    | 1.08       | 2.57          | 460                      |
| TP-303                     | 350                                    | 1.13       | 2.61          | 730                      |

\*Fixed during regression

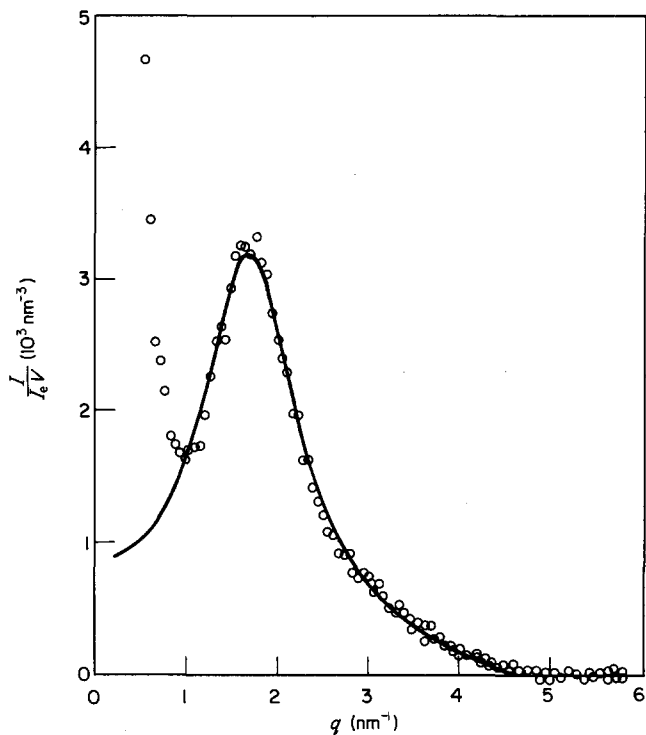


**Figure 8** SAXS curve and model fit for Sr SPS D

The dimensions and concentration of the aggregates do not seem to depend strongly on the cation or anion type. One interesting difference is observed between the carboxylated and sulphonated polystyrenes in that the effective layer thickness is lower for the carboxylated materials. This implies that this effective thickness is affected not only by the nature of the backbone but also by the nature of the ionic aggregate structure. Perhaps this is due to a difference in the density of chain placement on the aggregate surface.

In the SAXS data for the Surlyn<sup>R</sup> samples, the ionomer peak occurs at such a high angle that there is no region where the ionic phase scattering becomes negligible so as to allow a fit to the wide angle contribution. Therefore, the contributions from intraphase and thermal density fluctuations were approximated by a constant and included in the model fit. However, it became impossible to determine both the background level and the electron density difference independently. Therefore, the electron density

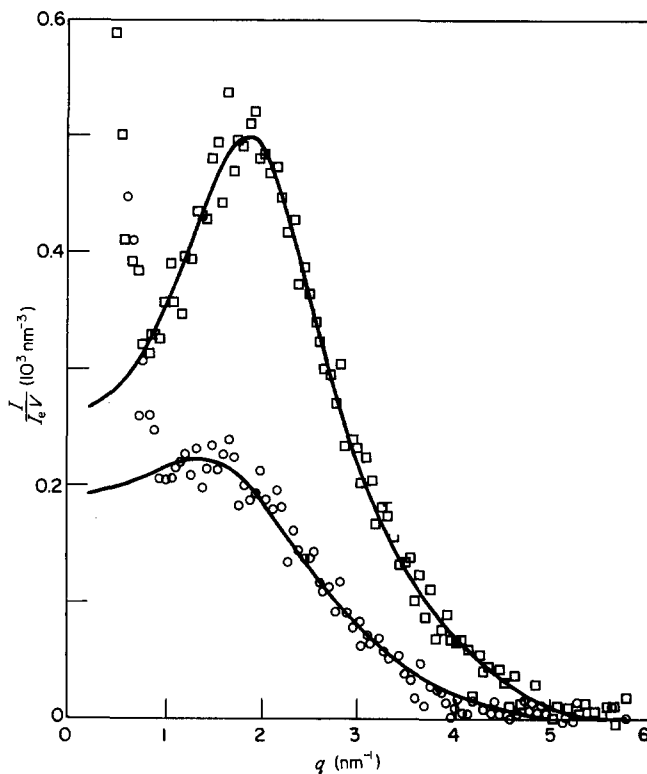


**Figure 9** SAXS curves and model fit for Zn CPS. Circles are for sample A and squares for sample D

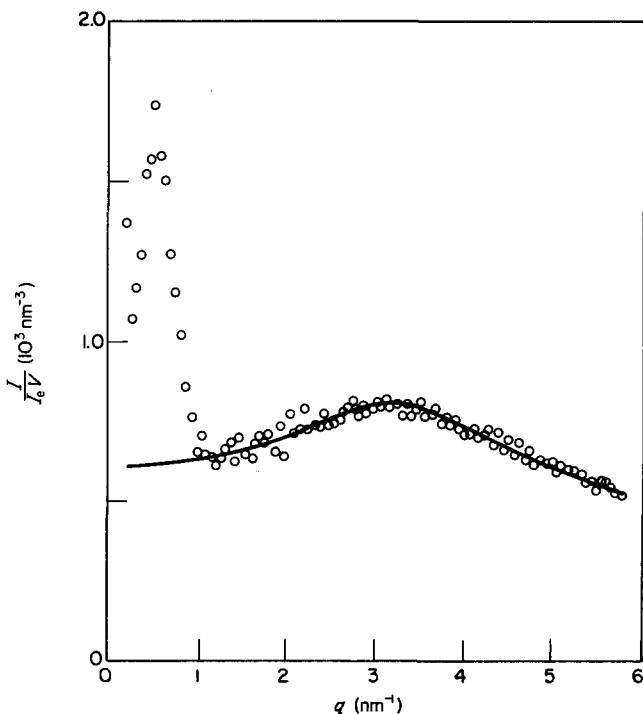


**Figure 10** SAXS curve and model fit for Surlyn<sup>R</sup> sample B10865

**Table 7** Model parameters for Zn SPS B vs. temperature

| Temp (°C) | $\rho_1$ (nm <sup>-3</sup> ) | $R_1$ (nm) | $R_{CA}$ (nm) | $v_p$ (nm <sup>3</sup> ) |
|-----------|------------------------------|------------|---------------|--------------------------|
| 25        | 119                          | 0.83       | 1.62          | 63                       |
| 100       | 117                          | 0.85       | 1.64          | 69                       |
| 140       | 121                          | 0.86       | 1.64          | 77                       |
| 180       | 122                          | 0.87       | 1.63          | 79                       |
| 220       | 128                          | 0.86       | 1.61          | 83                       |
| 260       | 127                          | 0.87       | 1.61          | 83                       |
| 280       | 109                          | 0.89       | 1.61          | 73                       |

**Table 8** Model parameters for Zn SPS D vs. temperature

| Temp (°C) | $\rho_1$ (nm <sup>-3</sup> ) | $R_1$ (nm) | $R_{CA}$ (nm) | $v_p$ (nm <sup>3</sup> ) |
|-----------|------------------------------|------------|---------------|--------------------------|
| 25        | 100                          | 0.82       | 1.45          | 28                       |
| 100       | 101                          | 0.84       | 1.46          | 29                       |
| 140       | 104                          | 0.85       | 1.47          | 32                       |
| 180       | 100                          | 0.86       | 1.45          | 32                       |
| 220       | 105                          | 0.86       | 1.46          | 33                       |
| 260       | 105                          | 0.88       | 1.43          | 32                       |
| 280       | 116                          | 0.85       | 1.44          | 33                       |

**Table 9** Model parameters for SPS acid C vs. temperature

| Temp (°C) | $\rho_1$ (nm <sup>-3</sup> ) | $R_1$ (nm) | $R_{CA}$ (nm) | $v_p$ (nm <sup>3</sup> ) |
|-----------|------------------------------|------------|---------------|--------------------------|
| 25        | 104                          | 0.97       | 1.70          | 166                      |
| 100       | 108                          | 0.98       | 1.73          | 193                      |
| 120       | 147                          | 0.97       | 1.57          | 329                      |
| 140       | 200                          | 0.93       | 1.74          | 502                      |
| 200       | 223*                         | 0.91       | 1.68*         | 662                      |
| 250       | 223*                         | 0.88       | 1.68*         | 600                      |

\* Fixed during regression

of the ionic phase was assumed to be that of crystalline zinc acetate dihydrate. It seemed reasonable to use this as a model structure since the aggregates here are so small and may indeed be of almost exclusively ionic character. Because of this assumption, one cannot put much confidence in the values of  $v_p$ , though the trends should still be meaningful. Also, the determination of the aggregate radius is essentially unaffected. From the apparent ionic phase dimensions and the zinc acetate model structure, one can calculate that for these materials, only about three or four carboxylate groups are in each aggregate. This corresponds to Eisenberg's definition of a multiplet, and to the qualitative estimate of ionic degree of association found by Marx. *et al.*<sup>4</sup>.

#### High temperature measurements

Five samples were chosen for SAXS study at elevated temperature. These were the same two zinc sulphonated polystyrenes used in the swelling experiments, a sample of the acid form of sulphonated polystyrene, a rubidium neutralized SPS and a Surlyn<sup>R</sup> ionomer. Tables 7–11 show the variation of the model parameters as a function of temperature.

First, the neutralized SPS samples will be discussed. The remarkable feature of these data is that there is essentially no change in the SAXS in going from 25°C to almost 300°C. In the Rb<sup>+</sup> sample, the parameters change somewhat at the highest temperature but this sample appeared degraded when removed from the sample chamber so the significance of those points is question-

able. Since these samples were readily compression moulded at 200°C, the implication is that viscous flow is possible even at temperatures where the ionic aggregates are stable in the absence of shear. It would be interesting to observe the SAXS of an ionomer while undergoing shear deformation.

The acid sample, in contrast, did show a significant decrease in the concentration of aggregates beginning at a temperature approximately equal to the matrix phase glass transition temperature. This suggests that perhaps the morphology of the control sample was metastable and reorganization took place as soon as the polymer chains became mobile. This transition is accompanied by an apparent increase in the electron density difference.

The data for the Surlyn<sup>R</sup> sample provide an interesting verification of the model. Figure 10 shows the SAXS curve for this sample at 25°C. The sharp peak at low angles here is due to the polyethylene crystallinity while the broad, low peak centred at  $\sim 3.2 \text{ nm}^{-1}$  is the ionomer peak. At 80°C, the polyethylene peak had sharpened and moved to lower angle as the annealing caused thickening and perfection of the crystalline lamellae. At 100°C, the crystallites had melted. At the same time, the ionomer peak had become a shoulder as shown in Figure 12. With the liquid-like model, this corresponds to a sudden increase in the average volume available to each aggregate as indicated in Table 11. This is just what would be expected since the volume available to the aggregates is only the amorphous region. When the crystallites melt, the volume of amorphous matrix increases. Such a change of shape of the scattering curve would not be predicted by the core-shell model where the structure giving rise to the scattering would be unaffected by a change in the crystalline portion.

## CONCLUSIONS

The water absorption studies can neither rule out nor support the proposed model. The problem with such studies is that one does not know enough about what happens to the ionic domains and the unaggregated ions upon water absorption. However, if the model is assumed

**Table 10** Model parameters for Rb SPS D vs. temperature

| Temp (°C) | $\rho_1$ (nm <sup>-3</sup> ) | $R_1$ (nm) | $R_{CA}$ (nm) | $v_p$ (nm <sup>3</sup> ) |
|-----------|------------------------------|------------|---------------|--------------------------|
| 25        | 126                          | 0.90       | 1.59          | 34                       |
| 120       | 122                          | 0.92       | 1.59          | 37                       |
| 150       | 125                          | 0.93       | 1.60          | 38                       |
| 200       | 129                          | 0.92       | 1.58          | 39                       |
| 250       | 105                          | 0.94       | 1.58          | 42                       |
| 295       | 98                           | 0.98       | 1.71          | 63                       |

**Table 11** Model parameters for B-10865 Surlyn vs. temperature

| Temp (°C) | $\rho_1$ (nm <sup>-3</sup> ) | $R_1$ (nm) | $R_{CA}$ (nm) | $v_p$ (nm <sup>3</sup> ) |
|-----------|------------------------------|------------|---------------|--------------------------|
| 25        | 225*                         | 0.42       | 0.77          | 10                       |
| 80        | 225*                         | 0.46       | 0.74          | 16                       |
| 100       | 225*                         | 0.53       | 0.74*         | 35                       |
| 120       | 225*                         | 0.55       | 0.74*         | 39                       |
| 140       | 225*                         | 0.56       | 0.74*         | 41                       |

\* Fixed during regression

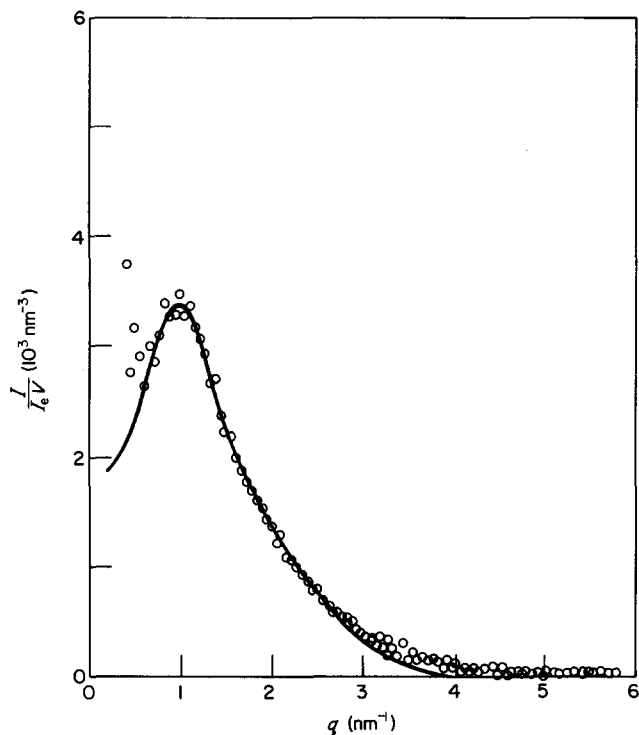


Figure 11 SAXS curve and model fit for sulphonated EPDM ionomer sample GL-47-C

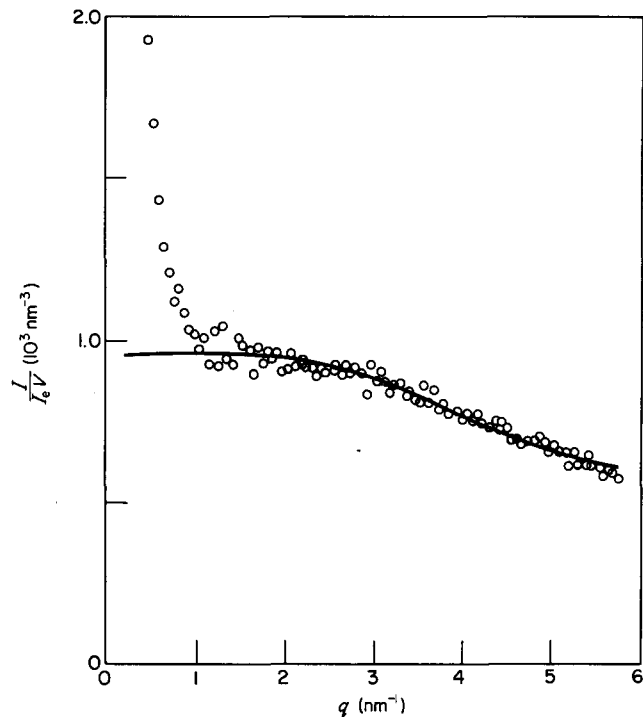


Figure 12 SAXS curve and model fit for Surlyn<sup>R</sup> sample B10865 at 100°C

to be correct, the results indicate that in the absorption process, the water does not all go into existing ionic domains with the same density as liquid water and with no change in the number of aggregates or the number of ionic groups in aggregates.

The model is generally applicable to the characteristic small angle X-ray scattering of ionomers and indicates some interesting differences in morphology between systems. For the ethylene/methacrylic acid ionomers, the ionic aggregates are quite small, corresponding roughly to Eisenberg's concept of a multiplet<sup>6</sup>. In other ionomers, the aggregates are somewhat larger, implying that some hydrocarbon material must be incorporated. The ionic aggregate size seems to depend most strongly on the nature of the polymer backbone and the type of bound anion but not on the nature of the neutralizing cation or the overall ion content of the material.

The ionic domains in all the materials studied at elevated temperature were quite thermally stable. In the sulphonated polystyrene zinc salts in particular, no significant change was observed either in the aggregate size or in the concentration of aggregates over a temperature range from 25°C to 290°C.

#### ACKNOWLEDGEMENTS

The authors wish to thank Dr Robert Lundberg, Dr Ilan Duvdevani and the late Dr Henry Makowski all of the Exxon Research and Engineering Company for providing

some of the materials for this investigation. We also wish to thank Dr Adi Eisenberg for making available the carboxylated polystyrene samples used in this study. Finally, the partial support of this research by the polymers section of the NSF Division of Materials Research through grant DMR 81-06888 and the Department of Energy through contract DE-AC02-81ER 10922 is gratefully acknowledged.

#### REFERENCES

- 1 Yarusso, D. J. and Cooper, S. L. *Macromolecules* 1983, **16**, 1871
- 2 Fujimura, M., Hashimoto, T. and Kawai, H. *Macromolecules* 1982, **15**, 136
- 3 MacKnight, W. J. and Earnest, Jr., T. R. *J. Polym. Sci.: Macromol. Rev.* 1981, **16**, 41
- 4 Marx, C. L., Caulfield, D. F. and Cooper, S. L. *Macromolecules* 1973, **6**, 344
- 5 Fujimura, M., Hashimoto, T. and Kawai, H. *Macromolecules* 1981, **14**, 1309
- 6 Eisenberg, A. *Macromolecules* 1970, **3**, 147
- 7 Lundberg, R. D. and Makowski, H. S. *Am. Chem. Soc. Adv. Chem.* 1980, **187**, 21
- 8 Lake, J. A. *Acta Crystallogr.* 1967, **23**, 191
- 9 Rathje, J. and Ruland, W. *Colloid Polym. Sci.* 1976, **254**, 358
- 10 Hendricks, R. W., Shaffer, L. B. et al. *J. Appl. Crystallogr.* 1978, **11**, 196
- 11 Fournet, G. *Compt. Rend.* 1949, **228**, 1421
- 12 Fournet, G. *ibid.* 1949, **229**, 1071
- 13 Fournet, G. *Acta Crystallogr.* 1951, **4**, 293
- 14 Born, M. and Green, H. S. *Proc. Roy. Soc. London* 1946, **A-188**, 10 10